HHS Public Access

Author manuscript

Nat Methods. Author manuscript; available in PMC 2015 June 01.

Published in final edited form as:

Nat Methods. 2014 December ; 11(12): 1233–1236. doi:10.1038/nmeth.3143.

An Improved Surface Passivation Method for Single-Molecule Studies

Boyang Hua[1], **Kyu Young Han**[2,3,4], **Ruobo Zhou**[2,3,10], **Hajin Kim**[5,6], **Xinghua Shi**[4,7], **Sanjaya C. Abeysirigunawardena**[8], **Ankur Jain**[1], **Digvijay Singh**[1], **Vasudha Aggarwal**[1], **Sarah A. Woodson**[8,9], and **Taekjip Ha**[1,2,3,4,7]

[1]Center for Biophysics and Computational Biology, University of Illinois at Urbana-Champaign, Urbana, Illinois, USA

[2]Department of Physics, University of Illinois at Urbana-Champaign, Urbana, Illinois, USA

[3]Center for the Physics of Living Cells, University of Illinois at Urbana-Champaign, Urbana, Illinois, USA

[4]Howard Hughes Medical Institute, Urbana, Illinois, USA

[5]School of Life Sciences, Ulsan National Institute of Science and Technology, Ulsan, Republic of Korea

[6]Center for Soft and Living Matter, Institute for Basic Science, Ulsan, Republic of Korea

[7]Institute for Genomic Biology, University of Illinois at Urbana-Champaign, Urbana, Illinois, USA

[8]T.C. Jenkins Department of Biophysics, Johns Hopkins University, Baltimore, Maryland, USA

[9]CMDB Program, Johns Hopkins University, Baltimore, Maryland, USA.

Abstract

We herein report a surface passivation method for *in vitro* single-molecule studies, which more efficiently prevents non-specific binding of biomolecules as compared to the polyethylene glycol surface. The new surface does not perturb the behavior and activities of tethered biomolecules. It can also be used for single-molecule imaging in the presence of high concentrations of labeled species in solution. Reduction in preparation time and cost is another major advantage.

[10]Present address: Department of Chemistry and Chemical Biology, Harvard University, Cambridge, Massachusetts, USA. Correspondence should be addressed to T.H. (tjha@illinois.edu).

Note: Supplementary information is available in the online version of the paper.

Author contributions

B.H. and T.H. designed the project, B.H., K.Y.H., R.Z., H.K. and X.S. performed the experiments, S.C.A and S.A.W provided the S4-rRNA complex and three other ribosomal protein samples, B.H., K.Y.H., R.Z., H.K., X.S., A.J., D.S., V.A. and T.H. analyzed the data, and B.H., K.Y.H., R.Z, H.K., X.S. and T.H. wrote the manuscript.

Competing financial interests

The authors declare no competing financial interests.

During the past two decades, single-molecule techniques have been greatly advanced and widely applied to biological sciences.[1–3] Nowadays, through wide-field fluorescence microscopy,[4] one can routinely record signals from hundreds of single biomolecules in parallel. One of the many merits of single-molecule techniques is that it avoids ensemble averaging and thus reveals intermediate states as well as heterogeneity in biomolecules that are otherwise hidden in conventional ensemble measurements. However, a population of non-specifically bound biomolecules on the imaging surface is difficult to filter out during analysis and sometimes alters results by their contribution to the overall statistical analysis. The polyethylene glycol (PEG) passivation[5,6] and protein blocking[7] are two most widely used surface passivation methods in single-molecule studies. Nevertheless, the PEG surface typically is only able to reject non-specific adhesion of biomolecules of low nanomolar concentrations while the protein-blocked surface is generally less effective in passivation.[8] This concentration range is too low for many physiologically relevant biomolecular interactions to take place since weak and transient interactions could exhibit dissociation constants (*KD*) in the micromolar range.[9] Several optical measurement techniques have been developed to detect single fluorophores at higher concentrations[10,11] but these methods would not achieve their maximum utility without better passivated surfaces. Here we report a greatly improved surface passivation method for single-molecule studies, which can reduce non-specific adsorption of biomolecules by typically 10-fold and up to 30-fold, depending on the system under study, as compared to the PEG surface while keeping biomolecular activities intact. The new method is also much less expensive in terms of time and reagent cost.

Revyakin *et al* suggested additional passivation steps with polysiloxane and Tween-20 on the basis of the PEG surface to improve surface passivation.[12] However, their method extends the PEG surface preparation time by additional 16 hours and leads to strong green background fluorescence requiring overnight laser bleaching. Inspired by the surface used by Helenius *et al*, which is passivated with hydrophobic coating materials and the surfactant F-127,[13] we tested eight different combinations of hydrophobic coating silanes and surfactants using Cy5-labeled DNA polymerase DinB[14] (Supplementary Fig. 1). With consideration of their passivation capacity as well as preparation time and cost, we chose dimethyldichlorosilane (DDS)-Tween-20 over other combinations. The scheme of the DDS-Tween-20 (DT20 for short) surface is illustrated (Fig. 1a). Tween-20 self-assembled onto the DDS-coated surface serves as the passivation layer while biotinylated bovine serum albumin (BSA) adsorbed before Tween-20 treatment is used to present biotin for specific tethering of biomolecules through the biotin-NeutrAvidin interaction. The autofluorescence of Tween-20 was negligible compared to typical organic fluorophores used for single-molecule imaging. The DT20 and PEG surfaces had similar density of fluorescence impurities although some impurities on the DT20 surface were diffusing (Supplementary Fig. 2 and Supplementary Video 1). We performed non-specific binding tests with fluorophore-labeled proteins or nucleic acids and counted the number of fluorescent spots per imaging area (~ 2500 μm^2) as the indicator of the level of non-specific binding. As a standard protocol for comparison, we washed out free biomolecules after incubation for spot counting (see online methods). Compared to the PEG surface, the DT20 surface consistently yielded much lower non-specific binding spot counts for Cy5-labeled DinB in a wide protein

concentration range (from 5 nM to 200 nM) at pH 8.0 (Fig. 1b). The improvement factor was about 30-fold regardless of the presence of NeutrAvidin, so a potential effect of different NeutrAvidin surface densities on the PEG vs DT20 surfaces can be ruled out as the source of the large difference in surface passivation (Supplementary Figs. 3 and 4). The large improvement in passivation capacity is due to the self-assembled Tween-20 layer rather than the non-specifically bound biotinylated BSA because without additional Tween-20 treatment the DDS-BSA surface had a much poorer passivation capacity (Supplementary Fig. 5). Successive binding tests on the same DT20 surface area indicated that non-specific binding primarily occurred to random positions although we cannot rule out the presence of surface defects that preferentially attract proteins (Supplementary Fig. 6). In addition to DinB, we also conducted non-specific binding tests for seven other proteins (Rep helicase, ribosomal proteins S4, S16, S17 and S20, and two antibodies) (Fig. 1c and Supplementary Fig. 7). Except for the antibodies, the DT20 surface exhibited at least 5-fold reduction in non-specific binding. We found that IgG is not highly sticky to the PEG surface, so the DT20 and PEG surfaces performed roughly the same in the IgG non-specific binding tests.

We next performed non-specific binding tests in the presence of high concentrations of fluorescent species in solution. A sub-diffraction limited focal spot generated by stimulated emission depletion (STED) microscope enabled us to image surface-tethered single molecules with high signal to background ratio in the presence of 100 nM streptavidin labeled with Alexa 594 (Fig. 1d).[15] In addition, the STED images obtained with labeled proteins in solution showed that the DT20 surface has reduced non-specific binding of streptavidin and protein G B1 domain (Fig. 1e and Supplementary Figs. 8 and 9).

We also compared the non-specific binding of a Cy3-labeled single-stranded (ss)DNA (34 nt). The DT20 surface prevented ssDNA from non-specific adsorption 10-fold more effectively under the two pH conditions we tested (pH 7.1 and pH 8.0; Fig. 1f and Supplementary Fig. 10) and maintained its passivation capacity with MgCl2 concentrations up to 80 mM (Supplementary Fig. 11). We tested additional fluorophores (Cy5, Abberior Star 635 and Atto 647N) linked to 18 nt ssDNA and found that all except Atto 647N displayed minimal non-specific binding (Fig. 1g). Atto 647N-labeled ssDNA bound to the surface and diffused rapidly (Supplementary Video 2) likely because its incorporation into the surfactant layer, consistent with severe non-specific adsorption of Atto 647N to lipid bilayers reported previously[16] and suggesting that other fluorophores that are known to strongly interact with the lipid bilayers [16] such as non-sulfonated Cy3 would not be suitable for use on the DT20 surface, if the fluorophore is conjugated to short DNA.

To test the biocompatibility of the DT20 surface with proteins and nucleic acids, we systematically compared the single-molecule data sets obtained on the DT20 and PEG surfaces. First, we measured the spontaneous transitions between the two stacked conformations of DNA Holliday junction (HJ) molecules[17] using single-molecule fluorescence resonance energy transfer (FRET)[18] (Fig. 2a). Single HJ FRET-time traces obtained from both surfaces showed clear two state transitions (Supplementary Fig. 12). The histograms of FRET efficiencies were nearly identical between the two surfaces in terms of the peak positions of the high and low FRET conformations and their ratio (Fig. 2b for 80

mM Mg^{2+} and Supplementary Fig. 13 for other Mg^{2+} concentrations). The transition rates between the high and low FRET conformations are known to increase with decreasing magnesium concentrations[17] and our analysis confirmed this and showed no substantial difference in the transition rates between the two surfaces (Fig. 2c).

For protein-nucleic acid interactions, we measured the repetitive looping activity of PcrA helicase on a partial duplex DNA with a 5' ssDNA overhang (Fig. 2d).[19] We observed the same sawtooth-shaped FRET-time traces, resulting from the repetitive PcrA translocation on the ssDNA overhang, as those previously obtained with the PEG surface at the same conditions (Fig. 2e).[19] To compare the translocation speed of PcrA on the two surfaces, we plotted the histograms of time intervals between two adjacent sudden drops (Δt) obtained from many single-molecule FRET-time traces at two ATP concentrations (Fig. 2f). Δt histograms obtained using the two surfaces gave almost identical distributions at each ATP concentration, indicating that the ssDNA translocation speed of PcrA was not much affected by the DT20 surface. Tests with the ribosomal protein S4-rRNA complex also confirmed the applicability to RNA-protein interactions (Supplementary Figs. 14 and 15).[20]

As a model system for protein-protein interactions, we examined the binding of DNA polymerase DinB to its processivity factor PCNA clamp at the concentration of 4 nM (Fig. 2g).[14] It has been shown that PCNA can promote the DinB loading to DNA at the replication fork through PCNA-DinB interactions,[14] so the formation of a ternary DinB-PCNA-DNA complex would result in a colocalized spot showing middle to high FRET value. In the Cy3 (green) and Cy5 (magenta) overlay images for both surfaces, we observed white to magenta colored spots, indicating the PCNA-DinB interaction was preserved on the DT20 surface (Fig. 2h). A lower density of spots on the PEG surface was due to a lower DNA coverage. Green spots were due to DinB bound to DNA with inactive or missing Cy5 because at ~ 4 nM non-specifically adsorbed DinB exists at a much lower surface density (Fig. 1b).

In this work, we immobilized biomolecules through biotinylated BSA that is non-specifically adsorbed to the DDS-coated surface prior to Tween-20 self-assembly. This method is compatible with long term imaging because less than 20 % of the biotinylated BSA detached from the DT20 surface over 2 hours (Supplementary Fig. 16). To test how long the non-covalently self-assembled Tween-20 layer may last, we measured non-specific binding of 500 nM Cy3-labeled ssDNA (34 nt) at pH 8.0 at different time points after the Tween-20 treatment. After 5 hours, the DT20 surface did not lose much effectiveness in rejecting non-specific binding (Supplementary Fig. 17).

In summary, we have devised and characterized a suitable surface passivation method for single-molecule biological studies which not only can substantially reduce non-specific binding but keep the native activities of biomolecules unaltered. Since this method spares the long PEGylation step[5] and uses inexpensive chemicals instead, it is also time and reagent economic. Therefore, we propose that this DT20 surface can supplement the PEG method and extend the reach of the powerful *in vitro* single-molecule experimental tools.

Online Methods

Preparation of the DDS-coated surface:[13]

Slides and coverslips cleaning procedure is the same as those for the regular PEG slides.[5] We mainly used KOH etching to clean and activate the surface. We also tried other methods, such as Piranha and oxygen plasma cleaning with similar results. Notice that prolonged burning is sometimes used to dry the surface. However, it may lead to dehydration of the surface hydroxyl groups.[21] Therefore, the burning step should be kept brief or eliminated. Dry the clean slides and coverslips thoroughly with N_2 and put them in a dry glass slide holder. (Move to the fume hood) Rinse the slide holder twice with hexane (Fisher Chemical, Spectranalyzed™). Add 75 mL hexane to the holder, and then add ~ 0.05 % (v/v) dichlorodimethylsilane (DDS, Aldrich, > 99.5 %) using a 1 ml syringe with needle. Put the needle tip under hexane to avoid air contact and inject DDS quickly since it is extremely reactive with moisture. Cover the holder with its cap and then wrap with aluminum foil tightly. Gently shake the holder at room temperature for 1 – 1.5 hours. (Move to the fume hood) Dump the hexane solution to a designated hexane-DDS mixture waste bottle. Rinse and sonicate the slides and coverslips with hexane for 1 min. Repeat the rinse and sonication step two more times. Air-dry the slides and coverslips with N_2. Put the slides and coverslips in 50 mL falcon tubes. Vacuum seal the tube in a food saver bag and store it at − 20 °C, where they should remain good for about 2 months. Besides hexane, cyclohexane (AR® (ACS), Macron Fine Chemicals™) is another suitable solvent we tested.

Using the DT20 slides

Take the slides and coverslips out from freezer and warm them up to room temperature. Then assemble them into flow chambers in the same manner as for the regular PEG slides. Flow in 50 μL 0.2 mg/mL biotinylated BSA (A8549, Sigma) in T50 buffer (20 mM Tris and 50 mM NaCl at pH 8.0) in each channel and incubate for 5 min. Flow in 100 μL 0.2 % Tween-20 (Fisher BioReagents™) in T50 buffer in each channel and incubate for 10 min. After this step, the NeutrAvidin and sample solutions can be added in the same way as for the regular PEG slides. A pure DT20 surface was made without embedded BSA or NeutrAvidin by skipping the steps of biotinylated BSA and NeutrAvidin incubation.

Non-specific binding tests

Non-specific binding on the PEG or DT20 surface was tested by imaging the slide surface and counting the fluorescence spots per imaging area (2500 μm^2) at varying concentrations of fluorophore-labeled biomolecules (proteins or nucleic acids). Unless specified otherwise, the biomolecules were incubated in the flow chamber for 3 – 5 min, depending on the biomolecules, before they were washed out by 150 μl T50 buffer followed by 50 μl imaging buffer (T50 buffer containing additional 4 mM Trolox, 0.8 % wt/vol glucose, 165 U/ml glucose oxidase and 2170 U/ml catalase).[22] Same incubation time was applied to the PEG and DT20 surfaces. For non-specific binding tests of four ribosomal proteins, 5 random areas spreading the entire flow channels were imaged; for the rest of the biomolecules, 10 – 15 random areas were imaged. The average and standard deviation of surface spot counts were used as the indicator of the level of non-specific binding. All the experiments were performed at room temperature (22 ± 1 °C).

DinB was labeled with Cy5 hydrazide (GE healthcare) through aldehyde tags.[14] Non-specific binding tests with or without NeutrAvidin on the surface were conducted in T50 buffer. T50 buffer (pH 8.0) was used in all non-specific binding tests unless specified otherwise. Rep was labeled with Cy5 maleimide (GE healthcare). Four ribosomal proteins (S4, S16, S17 and S20) were labeled with Cy3 maleimide (GE healthcare) and non-specific binding tests were conducted in a buffer containing 80 mM K-HEPES, 300 mM KCl and 20 mM MgCl2 at pH 7.6. IgG # 1 was a donkey anti-rabbit antibody (611-701-127, Rockland) labeled with Alexa 647 NHS ester (Invitrogen) and IgG # 2 was an Alexa 568-labeled goat anti-mouse antibody (A-11004, Invitrogen). Cy3-labeled ssDNA (34 nt) was purchased from IDT with the sequence of 5'-/Cy3/ CAGAATCCGGCTAGTACCTCAATATAGACTCCCT-3'. Non-specific binding tests of Cy3-ssDNA (34 nt) were also conducted at pH 7.1, in addition to pH 8.0. ssDNA (18 nt) was purchased from IDT with the sequence of 5'-/5AmMC6/GCCTCGCTGCCGTCGCCA/ 3biotin/-3'. This ssDNA (18 nt) was separately labeled with three different fluorophores, *i.e.* Cy5 NHS ester (GE healthcare), Abberior Star 635 NHS ester (Abberior) and Atto 647N NHS ester (Sigma).

Prism-based total internal reflection fluorescence (TIRF) imaging

The flow chamber was imaged under a prism-based TIRF microscope[23] equipped with 532 nm laser (Compass 315M, Coherent) and 633 nm laser (Research Electro-Optics) for Cy3 and Cy5 excitation, respectively. The fluorescence collected by a water immersion objective (NA 1.2, 60 ×, Olympus) was split into two channels by a dichroic beam splitter and recorded by EMCCD camera (IXon 897, Andor Technology) with the time resolution of 0.03 s or 0.1 s. The fluorescence emission filters used were a double-notch filter (Z532/633, Chroma) and a band pass filter (680 ± 20 nm, Chroma).

An averaged image of the first ten camera frames was generated by a custom IDL code and the fluorescence spots in the averaged image were identified and counted based on two criteria: 1) the fluorescence spot should be fit to a two-dimensional Gaussian within a predetermined fitting error to avoid including multiple molecules or aggregations into the analysis; 2) the intensity maxima should be greater than a predetermined threshold. The intensity threshold was kept the same for direct comparison between different surfaces. Some custom software and codes are available at https://cplc.illinois.edu/software and http://bio.physics.illinois.edu/HaMMy.asp while the rest can be provided upon request.

Preparation of the four ribosomal proteins

E. coli ribosomal protein S4 was labeled at residue 189 by site-directed mutagenesis of pET24b/rpS4_C32S as previously described.[20] Single cysteine residues were introduced in *E. coli* ribosomal proteins S16 (position 44) and S20 (position 23) through site-directed mutagenesis (QuikChange, Stratagene) of pET24b/rpS16 and pET24b/rpS20 vectors respectively.[24] Similarly, a natural cysteine in S17 was replaced with alanine (rpS17:C64A). These variant ribosomal proteins with single cysteine residues were over-expressed and purified by cation exchange chromatography using an UNO S6 column (BioRad) as described by Culver and Noller.[24] Isolated proteins were dialyzed overnight into storage

buffer 1 (80 mM K-Hepes, pH 7.6, 1 M KCl, 1 mM TCEP) with three buffer changes and stored at − 80 °C in 500 μL aliquots.

Purified proteins were pre-incubated in 1 ml of reaction buffer (80 mM K-Hepes, pH 7.6, 1 M KCl, 1 mM TCEP, 3 M urea) at 20 °C for 30 min, then reacted with a 6-fold molar excess of maleimide-linked Cy3 or Cy5 (GE Healthcare) at 20 °C for another 2 hours. The reactions were quenched by adding 50 ml 20 mM Tris-HCl, pH 7.0, 6 M urea and 6 mM 2-mercaptoethanol (20 mM KCl, final concentration). Excess unreacted dye was removed by ion exchange chromatography. Labeled proteins were dialyzed overnight against storage buffer 2 (80 mM K-Hepes, pH 7.6, 1 M KCl, 6 mM 2-mercaptoethanol) and stored at − 80 °C in a light-tight box. The concentration of the labeled proteins was determined from the absorbance at the absorption maxima for the respective cyanine dyes ($\varepsilon_{650,\ Cy5}$ = 250,000 $M^{-1}cm^{-1}$, $\varepsilon_{550,\ Cy3}$ = 150,000 $M^{-1}cm^{-1}$).

Single-molecule imaging by STED microscope

A flow chamber passivated by either PEG or DT20 was prepared as described earlier except that they did not have biotin and that for some experiments (Fig. 1d and Supplementary Fig. 8a), Alexa 594-labeled streptavidin with ~ 2:1 labeling ratio (S-32356, Invitrogen; hereinafter SA-A594) was first immobilized non-specifically to the DDS surface before 0.2 % Tween-20 in T50 buffer was added to passivate the surface. Confocal and STED imaging was performed with (Fig. 1d, e) or without (Supplementary Fig. 8) 100 nM SA-A594 in solution, and with 50 nM Alexa 594-labeled protein G B1 domain in solution (Supplementary Fig. 9). For each condition, at least 3 random areas spreading the entire flow channels were imaged.

A custom built STED microscope was used.[15] Light from a Ti:Sapphire laser (λ = 750 nm, Spectra Physics) was split up to use as STED and excitation beams. The excitation pulses were generated by a photonic crystal fiber (NKT photonics)[25] and spectrally filtered in the range of 565 ± 12 nm (Semrock). The STED pulses were stretched to ~ 300 ps by two glass rods (Casix) and a 100 m long fiber (OZ optics). The spatially filtered excitation and STED pulses were reflected by dichroic beam splitters (Chroma) with circular polarization (B. Halle Nachfl.) and focused onto the sample plane by an objective lens (NA 1.4 HCX PL APO 100 ×, Leica Microsystems). The lateral doughnut-shaped STED beam was made by a phase plate with a helical lamp pattern (RPC photonics). The fluorescence signal was collected by the same objective over the wavelength range of 600 – 640 nm (Chroma) and registered by an avalanche photo diode (Perkin Elmer) with a multimode fiber (Thorlabs). The scanning of the sample was accomplished by a piezo-stage and the laser powers of excitation and STED beam were 1.5 μW and 54 mW, respectively.

Holliday junction dynamics

The Holliday junction (HJ) was annealed by mixing four DNA strands (ordered from IDT) with the molar ratio 1:1:1:1 (final concentration ~ 10 μM each) in 10 mM Tris:HCl (pH 8.0) and 50 mM NaCl followed by slow cooling from 90 °C to room temperature for ~ 2 hours. The sequences of the four oligonucleotides are as follows:

5’-CCTCCCTAGCAAGCCGCTGCTACGG-3’; 5’-/Cy3/CCGTAGCAGCGCGAGCGGTGGG-3’;

5’-/biotin/CCCACCGCTCGGCTCAACTGGG-3’; 5’-CCCAGTTGAGCGCTTGCTAGGG/Cy5/-3’.

150 – 250 pM of Cy3 and Cy5-labeled HJ molecules were immobilized on either the PEG surface or DT20 surface. Surface immobilization was mediated by biotin-NeutrAvidin binding between biotinylated HJ, NeutrAvidin, and surface immobilized biotinylated BSA. Excess unbound HJ was flushed out of the sample chamber using 200 μl imaging buffer (20 mM Tris (pH 8.0), 10 – 80 mM MgCl2, 5 mM NaCl, 4 mM Trolox, 0.8 % wt/vol glucose, 165 U/ml glucose oxidase and 2170 U/ml catalase) and Cy3 and Cy5 intensities from single HJ were recorded by the TIRF microscope[23] with the time resolution of 0.03 s. More than 8000 molecules were used to construct each histogram and more than 500 time intervals were used to calculate each transition rate.

PcrA repetitive looping activity

Sequence of the partial duplex DNA used in this experiment is 5’-/Cy3/$(dT)_{40}$GCCTCGCTGCCGTCGCCA-3’+5’-/Cy5/TGGCGACGGCAGCGAGGC/biotin/-3’ (IDT). PcrA was purified from *Bacillus stearothermophilus* as described by Niedziela-Majka *et al*.[26] 100 pM PcrA reaction solution was prepared by diluting PcrA stock into imaging buffer (20 mM Tris (pH 8.0), 4 mM Trolox, 0.8 % wt/vol glucose, 165 U/ml glucose oxidase and 2170 U/ml catalase) with additional 10 mM KCl , 5 mM $MgCl_2$ and ATP at either 10 or 500 μM. Then this reaction solution was added into the chamber with surface-immobilized partial duplex DNA. The experiment was performed at room temperature and the images were recorded by the TIRF microscope[23] with the time resolution of 0.03 s. More than 800 cycles of repetitive FRET changes were used to construct each histogram.

DinB-PCNA binding

M. acetivorans PCNA, RFC (replication factor C) and DinB were expressed recombinantly in *E. coli* and purified as described previously.[14, 27] The DinB we used in this study contained an aldehyde tag at the N terminus and was labeled quantitatively with Cy3 hydrazide using the protocol we published recently.[14]

Firstly, Cy5-labeled DNA was added at a concentration of 200 pM, followed by a 5 min incubation and rinse procedure. This DNA construct contained a biotin tag at the 5’ of the primer, a template of $(dT)_{20}$, and a four-way junction on the distal side of the template.[14] This addition of DNA was repeated a few more times until the surface was homogeneously covered with DNA. Next, a mixture of 20 nM PCNA, 1 mM ATP and 100 nM RFC was added in a buffer at pH 8.0 referred to as imaging buffer containing 25 mM Tris, 5 mM $MgCl_2$, 0.8 % wt/vol glucose and 2 mM Trolox, followed by 5 min incubation. After repeating this step two more times, sample chambers were rinsed extensively with imaging buffer. Last, Cy3-labeled DinB was added into the chamber at a concentration of 4 nM, incubated for 5 min, and rinsed with imaging buffer. FRET imaging of individual immobilized molecules of Cy3-labeled DinB and Cy5-labeled DNA was carried out in

imaging buffer plus 1.0 mg/ml glucose oxidase and 1,404 U/ml catalase. The TIRF microscope[23] was used to record images at 0.03 s time resolution.

Supplementary Material

Refer to Web version on PubMed Central for supplementary material.

Acknowledgments

We thank B. Leslie, S. Syed, T. Ngo, F. Tritschler and Q. Xu for their helpful comments in data analyses and manuscript preparation. We thank J. Guan, C. Yu and S. Granick for the helpful discussions as well as generously letting us use the oxygen plasma cleaning machine and Piranha fume hood. We thank T. Le of H. Kim laboratory at Georgia Institute of Technology and H.R. Koh of S. Myong laboratory at the University of Illinois for performing independent tests of our protocols. We thank W. Cheng at University of Michigan for providing the Alexa 594-labeled protein G B1 domain sample. This work was supported by U.S. National Science Foundation grant (PHY 1430124 to T.H.) and U.S. National Institutes of Health grants (GM065367 and AG042332 to T.H. and GM60819 to S.A.W.). T.H. is an investigator of the Howard Hughes Medical Institute.

References

1. Kim H, Ha T. Rep. Prog. Phys. 2013; 76:016601. [PubMed: 23249673]
2. Patterson G, Davidson M, Manley S, Lippincott-Schwartz J. Annu. Rev. Phys. Chem. 2010; 61:345–367. [PubMed: 20055680]
3. Xie XS, Choi PJ, Li G-W, Lee NK, Lia G. Annu. Rev. Biophys. 2008; 37:417–444. [PubMed: 18573089]
4. Funatsu T, Harada Y, Tokunaga M, Saito K, Yanagida T. Nature. 1994; 374:555–559. [PubMed: 7700383]
5. Ha T, et al. Nature. 2002; 419:638–641. [PubMed: 12374984]
6. Heyes CD, Groll J, Moller M, Nienhaus GU. Mol. BioSyst. 2007; 3:419–430. [PubMed: 17533455]
7. Jeyachandran YL, Mielczarski JA, Mielczarski E, Rai B. J. Colloid Interface Sci. 2010; 341:136–142. [PubMed: 19818963]
8. Visnapuu M-L, Duzdevich D, Greene EC. Mol. BioSyst. 2008; 4:394–403. [PubMed: 18414737]
9. van Oijen AM. Curr. Opin. Biotechnol. 2011; 22:75–80. [PubMed: 21036593]
10. Loveland AB, Habuchi S, Walter JC, van Oijen AM. Nat. Methods. 2012; 9:987–992. [PubMed: 22961247]
11. Elting MW, et al. Opt. Express. 2013; 21:1189–1202. [PubMed: 23389011]
12. Revyakin A, Zhang ZJ, et al. Genes Dev. 2012; 26:1691–1702. [PubMed: 22810624]
13. Helenius J, Brouhard G, Kalaidzidis Y, Diez S, Howard J. Nature. 2006; 441:115–119. [PubMed: 16672973]
14. Shi X, et al. Nat. Methods. 2012; 9:499–503. [PubMed: 22466795]
15. Han KY, et al. Nano Lett. 2009; 9:3323–3329. [PubMed: 19634862]
16. Hughes LD, Rawle RJ, Boxer SG. PLOS ONE. 2014; 9:e87649. [PubMed: 24503716]
17. McKinney SA, Déclais A-C, Lilley DMJ, Ha T. Nat. Struct. Biol. 2002; 10:93–97. [PubMed: 12496933]
18. Ha T, et al. Proc. Natl. Acad. Sci. USA. 1996; 93:6264–6268. [PubMed: 8692803]
19. Park J, et al. Cell. 2010; 142:544–555. [PubMed: 20723756]
20. Kim H, et al. Nature. 2014; 506:334–338. [PubMed: 24522531]
21. Zhuravlev LT. Colloids Surf., A. 2000; 173:1–38.
22. Rasnik I, McKinney SA, Ha T. Nat. Methods. 2006; 3:891–893. [PubMed: 17013382]
23. Joo, C.; Ha, T. ch. 2. In: Selvin, P.; Ha, T., editors. Single molecule techniques: A Laboratory Manual. Cold Spring Harbor, NY; Cold Spring Harbor Laboratory Press; 2007. p. 3-36.
24. Culver GM, Noller HF. Methods Enzymol. 2000; 318:446–460. [PubMed: 10890005]

25. Han KY, Leslie BJ, Fei J, Zhang J, Ha T. J. Am. Chem. Soc. 2013; 135:19033–19038. [PubMed: 24286188]
26. Niedziela-Majka A, Chesnik MA, Tomko EJ, Lohman TM. J. Biol. Chem. 2007; 282:27076–27085. [PubMed: 17631491]
27. Chen Y-H, et al. J. Biol. Chem. 2005; 280:41852–41863. [PubMed: 16257971]

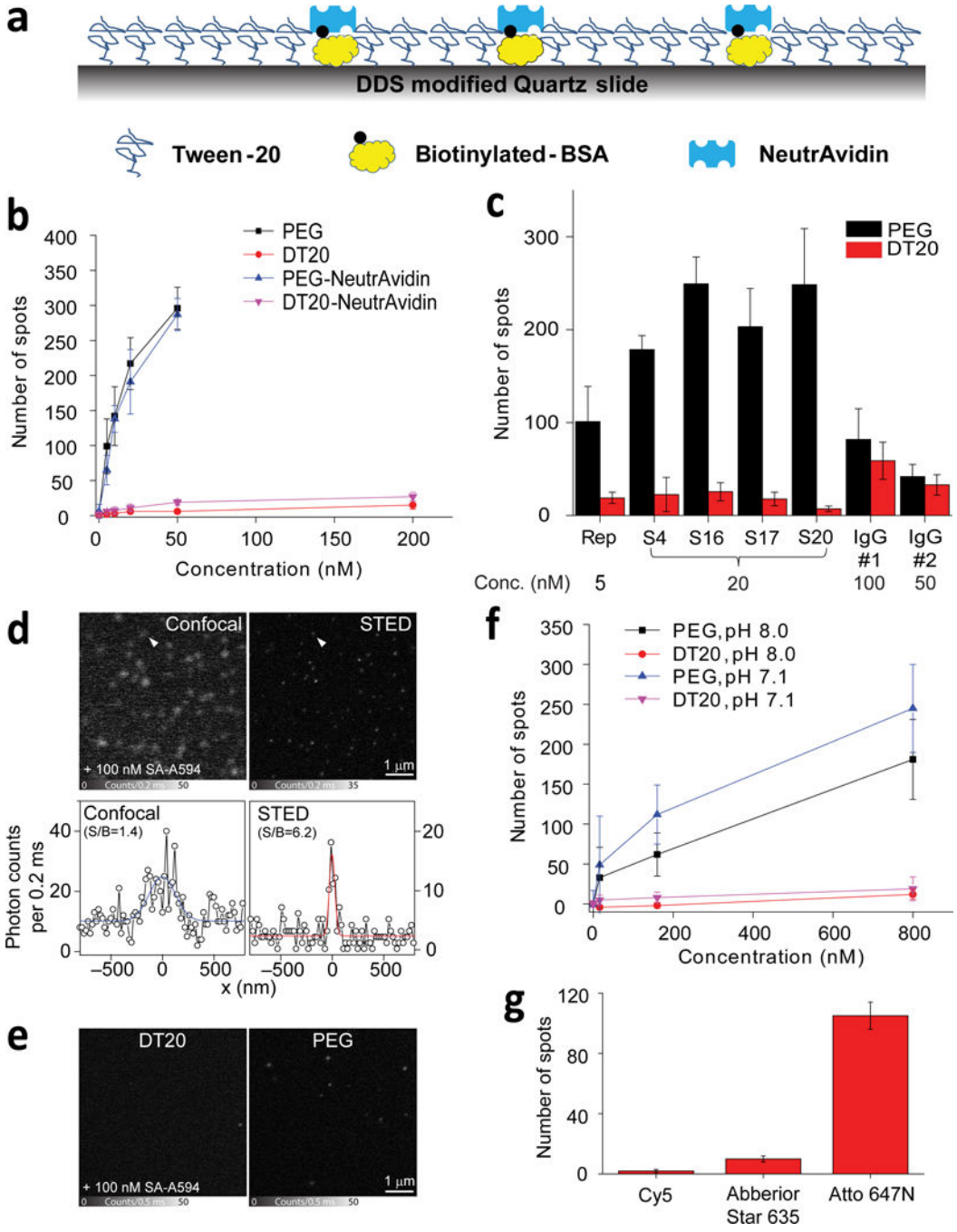

Figure 1.

The DT20 surface and its improved passivation capacity. (a) The schematics of the DT20 surface. (b) Non-specific binding of Cy5-labeled DinB on the DT20 and PEG surfaces, with and without NeutrAvidin, measured by the average surface spot counts of DinB over an imaging area of 2500 μm^2 at different concentrations of DinB. (c) The surface spot counts over an imaging area of 2500 μm^2 for non-specific binding of seven different proteins. Rep was labeled with Cy5 and tested at pH 8.0, four ribosomal proteins (S4, S16, S17 and S20) were labeled with Cy3 and tested at pH 7.6, IgG # 1 (611-701-127, Rockland) and IgG # 2

(A-11004, Invitrogen) were labeled with Alexa 647 and Alexa 568, respectively and tested at pH 8.0. (d) Fluorescence images of the surface (DT20) immobilized streptavidin-Alexa 594 (SA-A594) by confocal and STED microscope in the presence of 100 nM diffusing SA-A594 (top). Line profiles of single SA-A594 marked by white arrows (bottom). (e) Non-specific binding tests of the DT20 and PEG surfaces incubated with 100 nM SA-A594 by STED microscope. (f) Non-specific binding of Cy3-labeled ssDNA at different concentrations, measured at pH 8.0 and pH 7.1. (g) The surface spot counts over an imaging area of 2500 μm^2 for non-specific binding of 500 nM ssDNA (18 nt) labeled with three different fluorophores. All error bars in **Fig. 1 b, c, f, g** indicate standard deviation (s.d.).

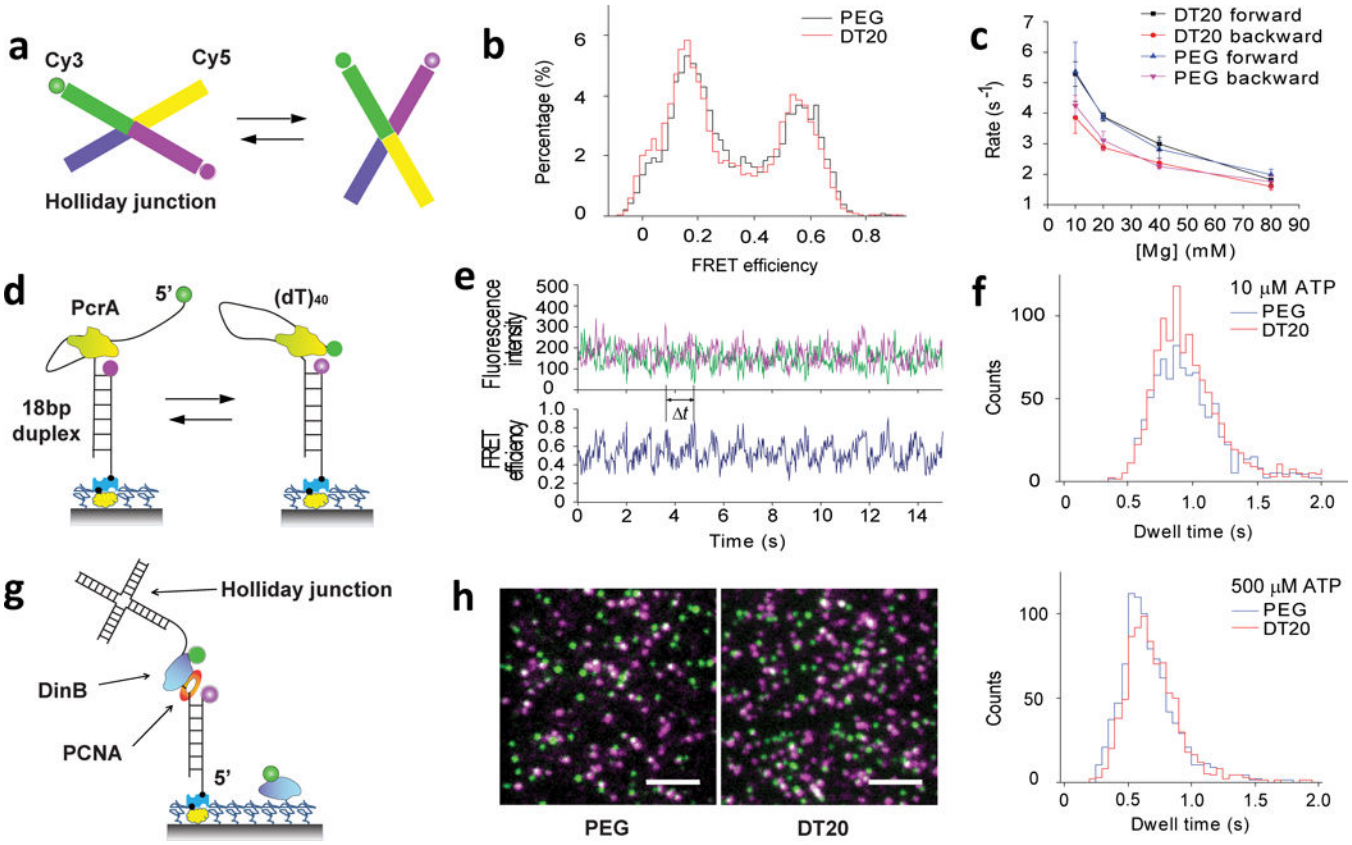

Figure 2.

Comparative analyses of biomolecular activities on the DT20 and PEG surfaces. (a) Detection of the dynamics of Holliday junction through FRET. (b) The FRET histograms of single Holliday junctions obtained at 80 mM Mg^{2+}. (c) The transition rates of Holliday junction decreases as the Mg^{2+} concentration increases. Error bars indicate s.d. (d) PcrA reeling causes the looping of 5' ssDNA tail. (e) Representative asymmetric sawtooth-shaped intensity and FRET-time traces of 5' ssDNA tail looping (green and magenta for Cy3 and Cy5 signals, respectively). (f) Δt histograms obtained at different ATP concentrations, 10 μM ATP (top) and 500 μM ATP (bottom). (g) The FRET signal distinguishes PCNA bound DinB from non-specifically bound DinB. A Holliday junction structure is used to prevent PCNA from sliding off the ssDNA region.[14] (h) Fluorescence images of DinB-PCNA interaction showing the overlay of the Cy3 (green) and Cy5 (magenta) channels for both surfaces. The scale bar indicates 4.5 μm.